

THE DOPING OF Eu^{2+} -INDUCED ENHANCEMENT IN DEFECT LUMINESCENCE OF ZnS

X. ZHANG*, L. WANG

School of Physics, Huaibei Normal University, Huaibei 235000, China

The doping of Eu^{2+} -induced enhancement in defect luminescence of ZnS (i.e., the 460 nm and 520 nm emission), is studied in this work. While the photoluminescence spectra show the 460 nm and 520 nm emission in both ZnS and ZnS:Eu phosphors, the photoluminescence excitation spectra show different excitation characteristics in the two phosphors. In ZnS phosphors, no excitation absorption signal is observed at the excitation wavelength $\lambda_{\text{ex}} > 337$ nm (the bandgap energy). In ZnS:Eu phosphors, however, the 365 nm and 410 nm excitation bands, which correspond respectively to the absorption of Eu^{2+} acceptor level and the intra-ion transition absorption of Eu^{2+} , appear remarkably. Compared with ZnS phosphors, the 460 nm and 520 nm emissions are increased in intensity by more than 10 times in ZnS:Eu phosphors and the 520 nm emission is relatively enhanced as well. The reason is analyzed. It's revealed from this work that the doping of Eu^{2+} enhances defect luminescence of ZnS from two aspects. First and most important, the excited levels of Eu^{2+} acceptor-bound exciton serve as the intermediate state for electron relaxation, which avoids the non-radiative electron transfer to the valence band and thus increases the 460 nm and 520 nm emissions. Second, the intra-ion transition absorption of Eu^{2+} and subsequent energy transfer to sulfur vacancy cooperatively lead to the relative enhancement of the 520 nm emission.

(Received May 30, 2015; Accepted September 4, 2015)

Keywords: ZnS, Eu^{2+} acceptor-bound excitons, Excited levels, Electron relaxation

1. Introduction

ZnS is an excellent luminescence host material. Usually, transition and rare-earth (RE) metal elements are doped in ZnS host to obtain efficient impurity-activated luminescence. It has been demonstrated by several works that the doping of transition and RE metal ions can promote the photoluminescence (PL) intensity in ZnS [1–5]. For example, Yang et al. reported that the emission intensity is increased by about 5–6 times by doping Ce, Y, Nd, Er and Tb metal ions in ZnS nanocrystallites [1]. Sridevi et al. reported that the fluorescence intensity of ZnS nanoparticles doped with La, Mn, Co and Ni metal ions are 5–6 times that of pure ZnS [2]. Very recently, it's reported that the PL intensity in ZnS can be enhanced due to the doping of Eu^{2+} [3–5]. Ashwini et al. observed that the PL intensity is enhanced with the increasing doping concentration of Eu^{2+} in ZnS: Eu^{2+} nanoparticles, and the reason is ascribed to the increasing defect sites and traps due to the Eu^{2+} doping [3, 4]. Ma et al. reported that the doping of Eu^{2+} promotes the emission intensity of bulk ZnS phosphors by 7–30 times, and the reason is explained as the formation of Eu^{2+} -related defect [5]. In short, the luminescence enhancement in Eu^{2+} -doped ZnS is ascribed to the introduced defects and traps in above works.

* Corresponding author: zhangxiaobo@chnu.edu.cn

In this work, Eu^{2+} are doped in ZnS host and the results of PL spectra show that the defect luminescence of ZnS is increased by more than 10 times in ZnS:Eu phosphors. The reason is analyzed. It's believed that electrons in the conduction band (CB) in ZnS:Eu phosphors are relaxed via the excited levels of Eu^{2+} acceptor-bound excitons, which avoids the non-radiative electron transfer to the valence band and thus increases the 460 nm and 520 nm emissions. Obviously, this conclusion is different with the explanation that defects and traps cause the luminescence enhancement in Eu^{2+} -doped ZnS in previous works [3-5].

2. Experimental details

Two phosphors, i.e., ZnS and ZnS:Eu phosphors, were prepared in this work. ZnS and ZnS:Eu phosphors were obtained by annealing the corresponding nanoparticle precursors, which were prepared beforehand by the co-precipitation method. The precipitation of ZnS nanoparticles was performed starting from homogeneous solutions of zinc acetate ($\text{Zn}(\text{CH}_3\text{COO})_2 \cdot 2\text{H}_2\text{O}$) at 0.3 M and thioacetamide (TAA) at 0.4 M. The two solutions were prepared in ultrapure water (18 M Ω). They were separately heated to 80 °C and acidified to control the decomposition of TAA that generated the sulfide anions. Then they were mixed in a batch reactor with no agitation. The ratio of Zn:S was 1:1.3 in mol. The reaction temperature and time were fixed at 80 °C and 30 min. After that, the hydrolytic reaction of TAA was terminated by rapidly cooling the solution < 10 °C in an ice bath. Then the cooled solution was centrifuged at 4000 rpm, washed three times with ultra pure water to eliminate TAA, and washed three times with isopropyl alcohol. The cleaned powders were dried in vacuum overnight at 80 °C until complete evaporation of the solvent was achieved. So the ZnS nanoparticles were prepared. For the preparation of ZnS:Eu nanoparticles, the only difference during the synthesis was adding $\text{Eu}(\text{NO}_3)_3$ to $\text{Zn}(\text{CH}_3\text{COO})_2$ solution. The molar ratio of $\text{Eu}^{3+}:\text{Zn}^{2+}$ was 3:100.

In fact, the as-made ZnS and ZnS:Eu nanoparticles had so faint emission that F-4500 fluorescence spectrometer cannot almost detect. To get stronger emission, the prepared ZnS and ZnS:Eu nanoparticles were annealed for 15 min. under the protection of sulfur and carbon reduction atmosphere at different temperatures. After rapid cooling down to room temperature, ZnS and ZnS:Eu phosphors were obtained.

The crystalline structure was characterized by X-ray powder diffraction (XRD) technique. The PL and excitation (PLE) spectra were recorded with a Hitachi F-4500 fluorescence spectrometer. All measurements were conducted at room temperature.

3. Results and discussion

3.1. Experimental results

Fig. 1 shows the XRD patterns of ZnS nanoparticle precursors and ZnS phosphors annealed at different temperatures. For ZnS nanoparticle precursors, three diffraction peaks, corresponding respectively to the (111), (220) and (311) plane of zincblende phase, appear obviously, indicating the pure cubic crystal structure of ZnS nanoparticles. For ZnS phosphors, however, the mixed phases of cubic and hexagonal but mainly cubic appear, meaning the phase transition to hexagonal during the annealing.

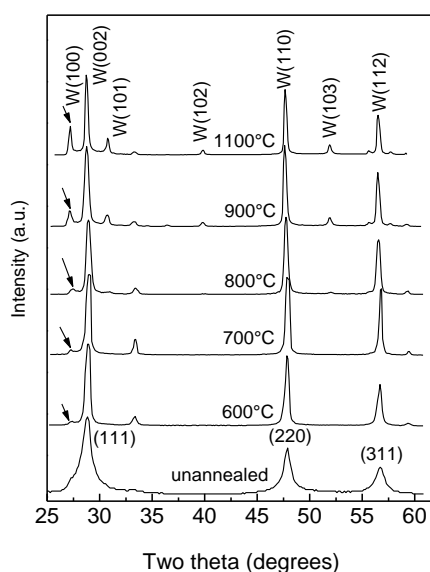


Fig. 1 XRD patterns of ZnS nanoparticle precursors and ZnS phosphors annealed at different temperatures. The occurrence of the (100) planes of hexagonal phase (marked with an arrow) indicates the structure transition of ZnS phosphors at annealing temperature > 600 °C.

A blue emission band centered at 460 nm and a green emission band centered at 520 nm, consist of the PL spectra of ZnS (Fig. 2(a)) and ZnS:Eu (Fig. 2(c)) phosphors. The 460 nm emission is the well-known self-activated (SA) luminescence of ZnS and the SA center is related to the Zn^{2+} vacancies [6, 7]. The 520 nm emission is assigned to the electron transfer from sulfur vacancies to interstitial sulfur states [8]. So, both the 460 nm and 520 nm emissions belong to defect luminescence of ZnS.

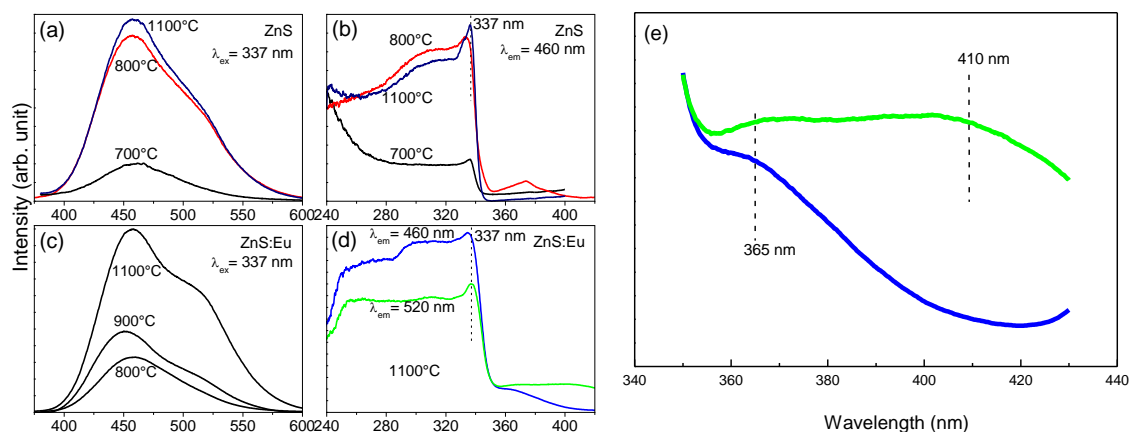


Fig. 2 PL and PLE spectra of ZnS (Fig. 2(a) and (b), respectively) and ZnS:Eu (Fig. 2(c) and (d), respectively) phosphors annealed at different temperatures. ZnS:Eu phosphors in Fig. 2(d) are annealed at 1100 °C. Fig. 2(e) is the enlargement of Fig. 2(d) in the wavelength range from 350 to 430 nm.

Fig. 2 (b) and (d) show the PLE spectra of ZnS and ZnS:Eu phosphors, respectively. A common excitation peak at 337 nm (3.68 eV), which corresponds to the absorption of the near

band-edge free excitons of ZnS, is observed for both ZnS and ZnS:Eu phosphors. However, different excitation characteristics appear in the long wavelength range in two phosphors: in ZnS phosphors, there is no excitation signal at the excitation wavelength $\lambda_{\text{ex}} > 337$ nm (Fig. 2 (b)); while in ZnS:Eu phosphors, however, two excitation bands centered at 365 nm and at 410 nm, which are respectively assigned to the electronic transition from the Eu^{2+} acceptor level to the conduction band of ZnS [9] and the $4f^7 \rightarrow 4f^6 5d^1$ of Eu^{2+} ions [9, 10], appear remarkably (Fig. 2(d)). Furthermore, the 365 nm and 410 nm excitation band contributes respectively to the 460 nm and 520 nm emission (Fig. 2(e)), which is quite consistent with the excitation characteristics of Eu^{2+} in ZnS: Eu^{2+} nanowires [9]. So, it's convincing to conclude that Eu^{2+} ions have been doped into ZnS:Eu phosphors.

To further reveal how the doped Eu^{2+} ions influences the 460 nm and 520 nm emissions, Fig. 3 shows the PL spectra of ZnS:Eu phosphors excited at different λ_{ex} ($\lambda_{\text{ex}} = 410, 390, 370, 350, 330$ nm). For comparison, the PL spectra of ZnS phosphors excited at 330 nm are also shown. Compared with ZnS phosphors, the intensities of 460 nm and 520 nm emissions are increased by more than 10 times in ZnS:Eu phosphors, and the 520 nm emission is more prominent in the spectra in ZnS:Eu phosphors, i.e., the 520 nm emission is relatively enhanced in ZnS:Eu phosphors. Except that, it's also worth noting that the 520 nm emission keeps almost unchanged in ZnS:Eu phosphors with the λ_{ex} varying from 410 nm, 390 nm, 370 nm, to 350 nm.

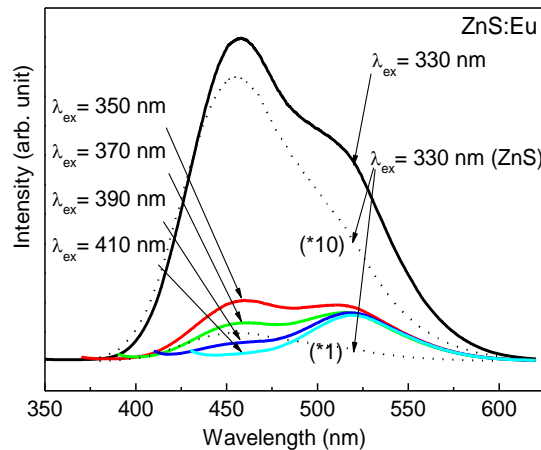


Fig. 3 PL spectra of ZnS:Eu phosphors excited at different wavelength (the solid lines). The dash lines represent the PL spectra of ZnS phosphors excited at 330 nm with 10 times and without enlargement. ZnS and ZnS:Eu phosphors here are annealed at 1100 °C.

3.2. Discussion

At the 330 nm excitation, the intensities of 460 nm and 520 nm emissions are increased dramatically in ZnS:Eu phosphors, which is ascribed to the electron relaxation via the excited levels of Eu^{2+} acceptor-bound excitons. As demonstrated in Fig. 2(d), the occurrence of the 365 nm excitation band proves the formation of Eu^{2+} isoelectronic acceptor level in ZnS:Eu phosphors. Therefore, holes are readily bound with electrons near the Eu^{2+} acceptor and thus, Eu^{2+} acceptor-bound excitons are formed [9]. It's believed that the excited levels of Eu^{2+} acceptor-bound excitons serve as the intermediate state for electron relaxation, that is, electrons in the conduction band (CB) are relaxed to the excited levels of Eu^{2+} acceptor-bound exciton first and then to the upper levels of 460 nm and 520 nm emissions. In ZnS phosphors, however, electrons in the CB are

directly transferred to the valence band (VB) non-radiative. So, the electron relaxation via the excited levels of Eu^{2+} acceptor-bound excitons avoids the non-radiative electron transfer to the VB and thus increases the 460 nm and 520 nm emissions. That explains the much stronger emissions in ZnS:Eu phosphors than in ZnS phosphors. The different electronic relaxation processes in two phosphors are illustrated in Fig. 4(a).

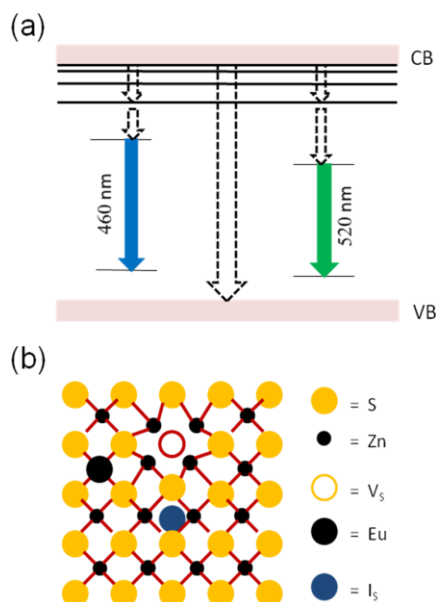
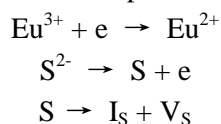


Fig. 4 (a) Different electron relaxation in ZnS and ZnS:Eu phosphors. The arrows in dash line represent electron relaxation and the black thick lines represent the excited levels of Eu^{2+} acceptor-bound excitons. In ZnS phosphors, electrons in the CB are directly relaxed to the valence band non-radiative, while ZnS:Eu phosphors, they are relaxed to the excited levels of Eu^{2+} acceptor-bound exciton first and then to the upper levels of 460 nm and 520 nm emissions. (b) Schematics of Eu^{2+} ions substituting Zn^{2+} and geminate generation of sulfur vacancy (V_S) and interstitials (I_S) near Eu^{2+} ions in ZnS:Eu phosphors.

Except the dramatic intensity increase in the 460 nm and 520 nm emissions, the 520 nm emissions is relatively enhanced in ZnS:Eu phosphors, which is ascribed to the intra-ion transition absorption of Eu^{2+} and subsequent energy transfer to sulfur vacancy. During the thermal annealing process, Eu^{3+} ions can be reduced to Eu^{2+} by obtaining electrons from the surrounding S^{2-} ions. And S^{2-} ions, after losing electrons, become S atoms, which will subsequently diffuse into the lattice interstitial, thus leaving vacancy on the site position. The reactions are as follows:



So sulfur vacancy (V_S) and interstitial (I_S) atoms are generated in pairs and located near Eu^{2+} ions in ZnS:Eu phosphors (see Fig. 4(b)). In that case, the excitation energy absorbed due to the intra-ion transition of Eu^{2+} can be efficiently transferred to sulfur vacancy because of the short distance between Eu^{2+} and sulfur vacancy, leading to the enhanced 520 nm emission. That's why the 520 nm emission is relatively enhanced in ZnS:Eu phosphors at the 330 nm excitation. It also explains the identity of the 520 nm emission at the varying λ_{ex} of from 410 nm, 390 nm, 370 nm to 350 nm because of the absorption saturation of Eu^{2+} intra-ion transition. Therefore, the intra-ion

transition absorption of Eu^{2+} and subsequent energy transfer to sulfur vacancy cooperatively lead to the relative enhancement of the 520 nm emission in ZnS:Eu phosphors.

4. Conclusions

The doping of Eu^{2+} -induced enhancement in defect luminescence of ZnS, is studied in this work. For this purpose, ZnS and ZnS:Eu phosphors were prepared by annealing the nanoparticle precursors. Different excitation characteristics are exhibited in the PLE spectra of two phosphors. While there is no excitation absorption signal at $\lambda_{\text{ex}} > 337$ nm in ZnS phosphors, the 365 nm and 410 nm excitation band, which corresponds respectively to the absorption of Eu^{2+} acceptor level and to the intra-ion transition absorption of Eu^{2+} , appear remarkably in ZnS:Eu phosphors. Compared with ZnS phosphors, the 460 nm and 520 nm emissions are increased in intensity by more than 10 times in ZnS:Eu phosphors, and the 520 nm emission is also relatively enhanced. The reason is analyzed. It's believed that the doping of Eu^{2+} enhances defect luminescence of ZnS in ZnS:Eu phosphors from two aspects. First and most important, the excited levels of Eu^{2+} acceptor-bound exciton serve as the intermediate state for electron relaxation, which avoids the non-radiative electron transfer to the VB and thus increases the 460 nm and 520 nm emissions. Second, the intra-ion transition absorption of Eu^{2+} and subsequent energy transfer to sulfur vacancy cooperatively lead to the relative enhancement of the 520 nm emission.

Acknowledgments

This study was financially supported by Collaborative Innovation Center of Advanced Functional Materials (No. XTZX103732015014) and the Natural Science Research Key Project of Anhui Province' University (No. KJ2010A303).

References

- [1] P Yang, M Lü, D Xü, D Yuan, G Zhou, J. Lumin., **93**, 101 (2001).
- [2] D Sridevi, KV Rajendran, Chalcogenide Lett., **7**, 397 (2010).
- [3] K Ashwini, C Pandurangappa, Nagabhushana BM, Phys. Scripta, **85**, 065706 (2012).
- [4] K Ashwini, C Pandurangappa, Opt. Mater., **37**, 537 (2014).
- [5] L Ma, K Jiang, X Liu, W Chen, J. App. Phys., **115**, 103104 (2014).
- [6] R Vacassy, SM Scholz, J Dutta, CJG Plummer, R Houriet, H Hofmann, J. AM. CERAM. SOC., **81**, 2699 (1998).
- [7] AD Dinsmore, DS Hsu, SB Qadri, JO Cross, TA Kennedy, HF Gray, BR Ratna, J. App. Phys., **88**, 4985 (2000).
- [8] X Wang, J Shi, Z Feng, M Li, C Li, Phys. Chem. Chem. Phys., **13**, 4715 (2011).
- [9] BC Cheng, ZG Wang, Adv. Funct. Mater., **15**, 1883 (2005).
- [10] W Chen, JO Malm, V Zwiller, Y Huang, S Liu, R Wallenberg, JO Bovin, L Samuelson, Phys. Rev. B, **61**, 11021 (2000).